**SUPPLEMENTARY MATERIALS**

Yunjong Lee[1-3,5], Senthilkumar S. Karuppagounder[1,3,5], Joo-Ho Shin[1,3,5,6], Yun-Il Lee[1,3,7], Han Seok Ko[1,3,8], Debbie Swing[9], Haisong Jiang[1,3,5], Sung-Ung Kang[1,3,5], Byoung Dae Lee[1,3,10], Ho Chul Kang[1,3,11], Donghoon Kim[1,3,8], Lino Tessarollo[9], Valina L. Dawson[1,2,3,4,5,*], and Ted M. Dawson[1,3,4,5,*]

[1]Neuroregeneration and Stem Cell Programs, Institute for Cell Engineering, Departments of [2]Physiology, [3]Neurology, and the [4]Solomon H. Snyder Department of Neuroscience, the Johns Hopkins University School of Medicine, Baltimore, MD 21205, USA

[5]Adrienne Helis Malvin Medical Research Foundation, New Orleans, LA 70130-2685, USA
[6]Division of Pharmacology, Department of Molecular Cell Biology
Sungkyunkwan University School of Medicine, Samsung Biomedical Research Institute, Suwon, South Korea

[8]Diana Helis Henry Medical Research Foundation, New Orleans, LA 70130-2685, USA

[9]Neural Development Section, Mouse Cancer Genetics Program, Center for Cancer Research, National Cancer Institute, Frederick, MD 21702,

[11]Department of Physiology, Ajou University School of Medicine, Suwon, Korea

[7]Present Address: Daegu Kyeongbuk Institute of Science and Technology, Daegu City, South Korea
[10]Present Address: Age-Related and Brain Disease Research Center, Department of Neuroscience, Kyung Hee University, Seoul, South Korea

**SUPPLEMENTARY FIGURES**

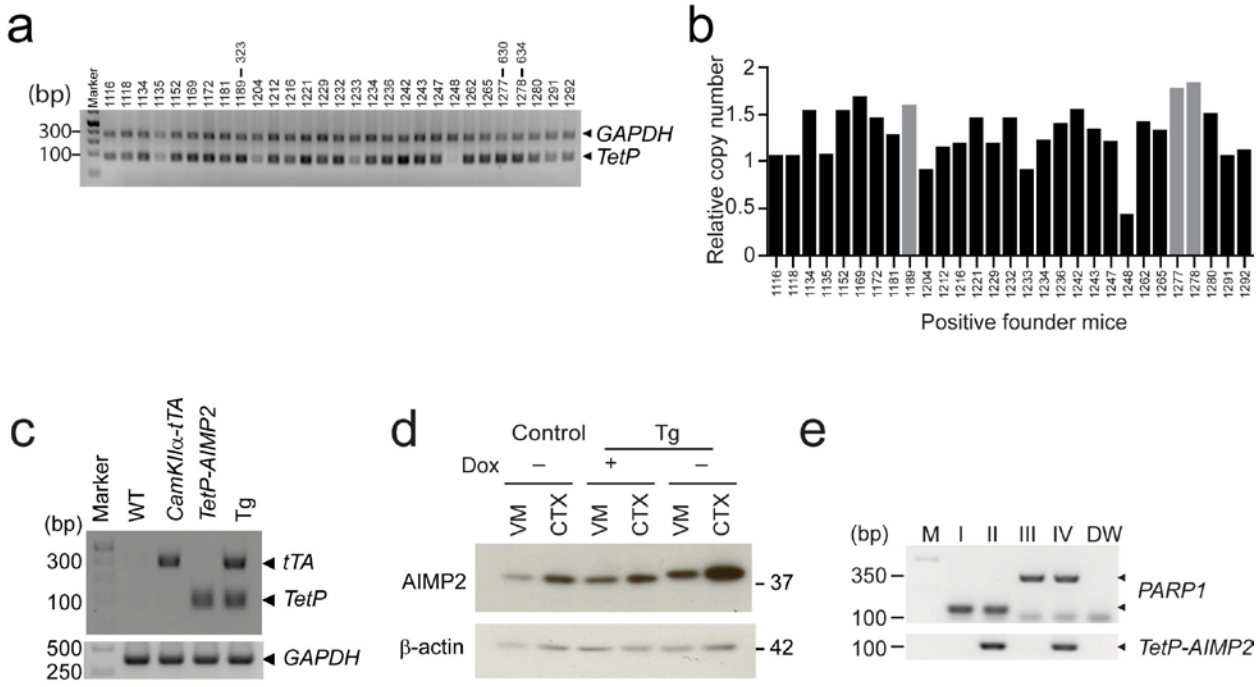


**Supplementary Fig. 1**

(a) Representative PCR genotyping of *TetP-AIMP2* and *GAPDH* using tail genomic DNA from founder mice with reduced cycle number for copy number comparison. GAPDH PCR was used as a genomic DNA loading control.

(b) Quantification of TetP-AIMP2 band intensities normalized to GAPDH for each founder mouse. High copy founder lines used for evaluating AIMP2 expression by mating with *CamKIIα-tTA* driver line are indicated with gray bars.

(c) Representative genotyping PCR for *TetP-AIMP2* and *CamKIIα-tTA* using tail genomic DNA. Tg denotes double positive mice for *TetP-AIMP2* and *CamKIIα-tTA*. GAPDH PCR was used as an internal control.

(d) Western blot analysis of AIMP2 induction in CTX and VM of *AIMP2* transgenic mice. AIMP2 induction was achieved in the CTX and VM of *TetP-AIMP2/CamKII*$\alpha$*-tTA* bigenic mice and suppressed by feeding the transgenic mice with doxycycline (Dox) food.

(e) Representative genotyping PCR for *TetP-AIMP2* and *PARP1* alleles using tail genomic DNA from indicated genotypes (I, control; II, *TetP-AIMP2*; III, *PARP1* KO; IV, *PARP1* $^{-/-}$/*TetP-AIMP2*). The upper band in PARP1 PCR is for mutant *PARP1* allele and lower band is for wild type allele. Full length blots are presented in Supplementary Figure 14 (d).

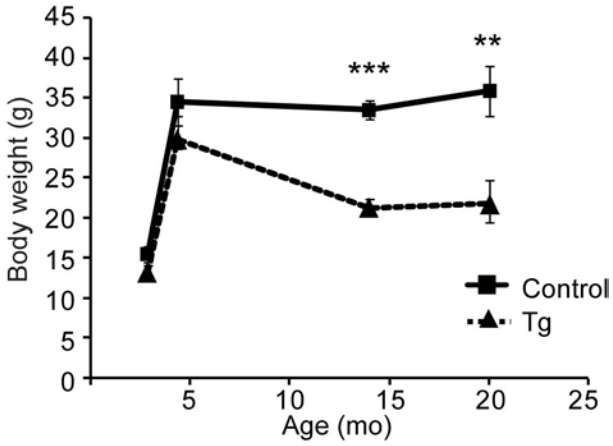


**Supplementary Fig. 2**

Assessment of body weight of *AIMP2* transgenic and controls (*n* = 8 for Control and *n* = 5 for Tg at 3 months, *n* = 6 per group at 4-5 months, *n* = 11 for Control and *n* = 5 for Tg at 14 months, *n* = 7 for Control and *n* = 7 for Tg at 20 months)

Quantified data are expressed as mean ± s.e.m., $^{**}p < 0.01$, $^{***}p < 0.001$, unpaired two-tailed Student's *t* test for *AIMP2* transgenics and controls of the same age group.

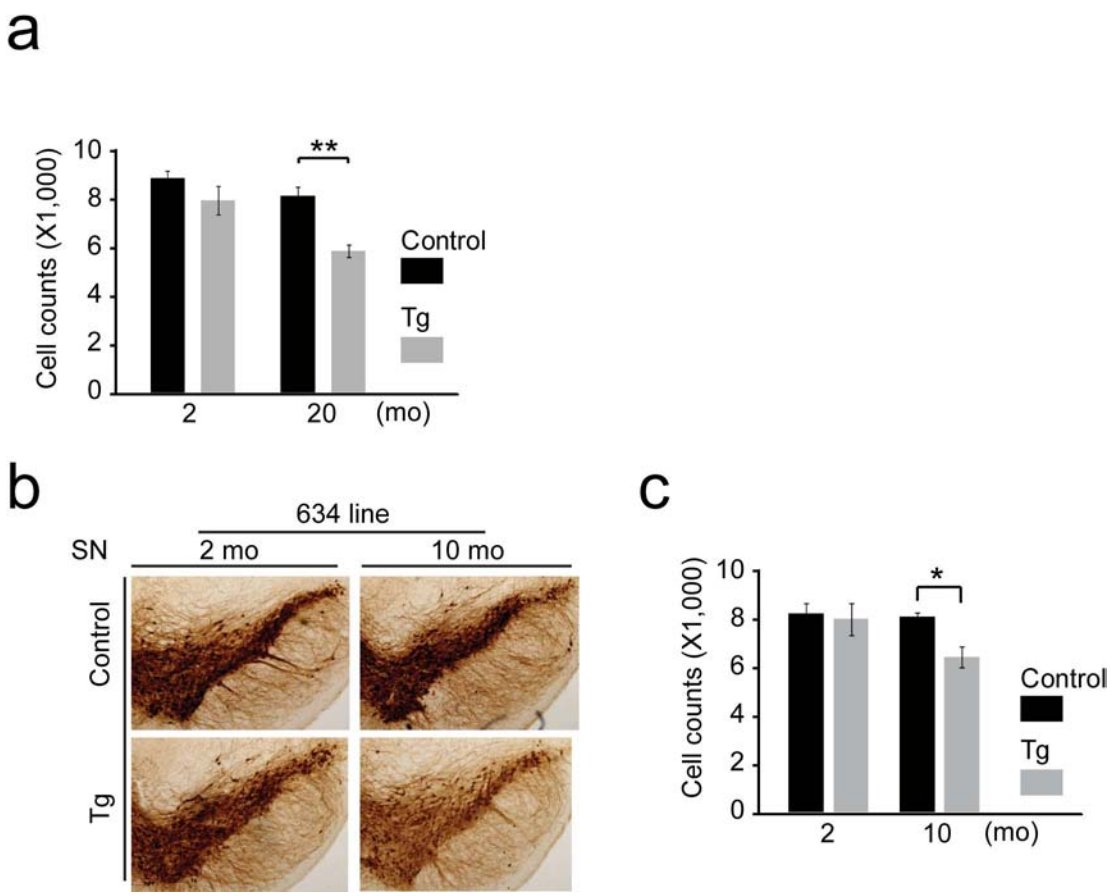


**Supplementary Fig. 3**

(a) Stereological assessment of TH positive neurons in the VTA of *AIMP2* transgenic and age matched littermate control mice (n = 5 Control, n=4 Tg at 2-3 months; n = 4 per group at 20 months)

(b) Representative anti-TH immunohistochemistry of the ventral midbrain of 2 month- and 10 month-old *AIMP2* transgenic (line 634) and littermate control.

(c) Stereological assessment of TH positive dopamine neurons in the substantia nigra (SN) of *AIMP2* transgenic (line 634) and age matched littermate control mice (n = 5 Control, n = 4 Tg at both age groups).

Quantified data are expressed as mean ± s.e.m., $*P < 0.05$, ANOVA test followed by Student-Newman-Keuls post-hoc analysis.

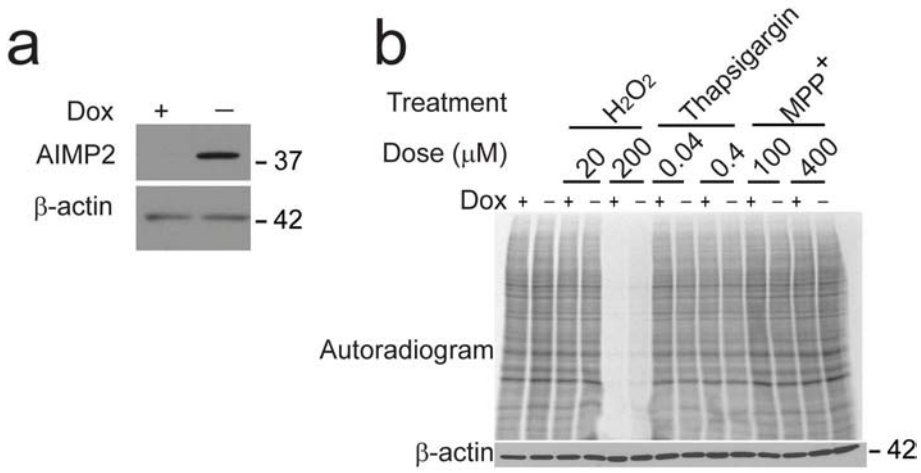


**Supplementary Fig. 4**

(a) Western blot analysis of AIMP2 induction in tet-off AIMP2-inducible PC12 cell line with removal of doxycycline (Dox –). β-actin serves as a loading control.

(b) Autoradiogram assessment of newly synthesized proteins ($^{35}$S methionine-incorporated proteins) with or without AIMP2 induction in the tet-off AIMP2 inducible PC12 cells that were grown in $^{35}$S methioine containing media for 10 minutes with increasing concentrations of $H_2O_2$, thapsigargin, or $MPP^+$. β-actin serves as a loading control. Full length blots are presented in Supplementary Figure 14.

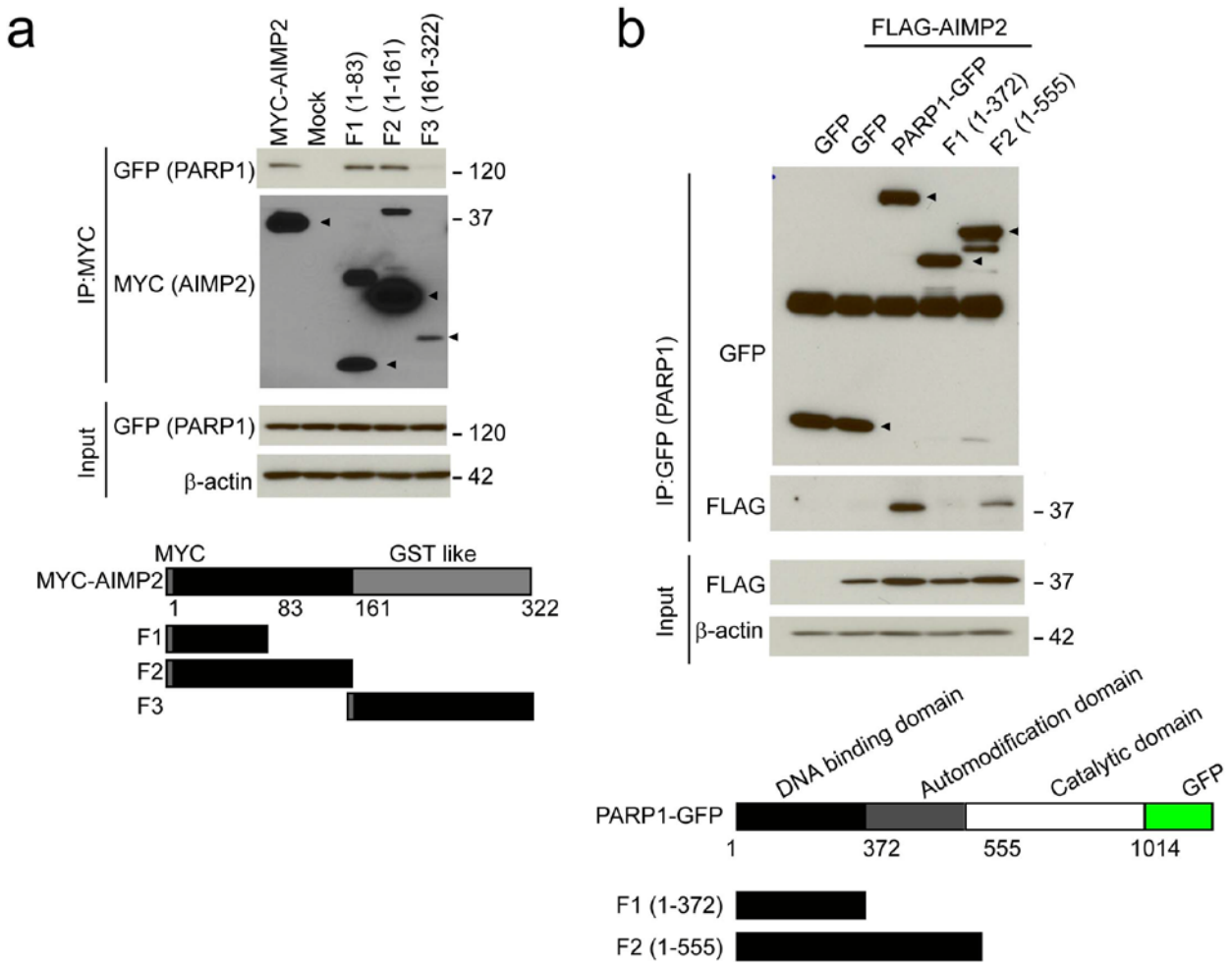


**Supplementary Fig. 5**

(a) Mapping of AIMP2 protein domains that interact with PARP1. Co-immunoprecipitation of PARP1-GFP and AIMP2-MYC from SH-SY5Y cells transfected with mock, MYC-tagged WT AIMP2 (Full length), or MYC-tagged AIMP2 deletion mutants containing amino acids 1-83, 1-161, or 161-322 of AIMP2. Immunoprecipitated AIMP2 WT and deletion mutants are indicated by filled triangles. The schematic of the AIMP2 domains and deletion mutants is shown in the bottom panel.

(b) Mapping of PARP1 domains that interact with FLAG-AIMP2. Co-immunoprecipitation of AIMP2 and PARP1-GFP from SH-SY5Y cells cotransfected with FLAG-AIMP2 and EGFP-PARP1 WT, and its deletion mutants containing only amino acids 1-372, and 1-555 of PARP1.

PARP1-GFP WT and mutants are indicated with filled triangles. The schematic of PARP1 domains and the mutants is shown in the bottom panel. Full length blots are presented in Supplementary Figure 14.

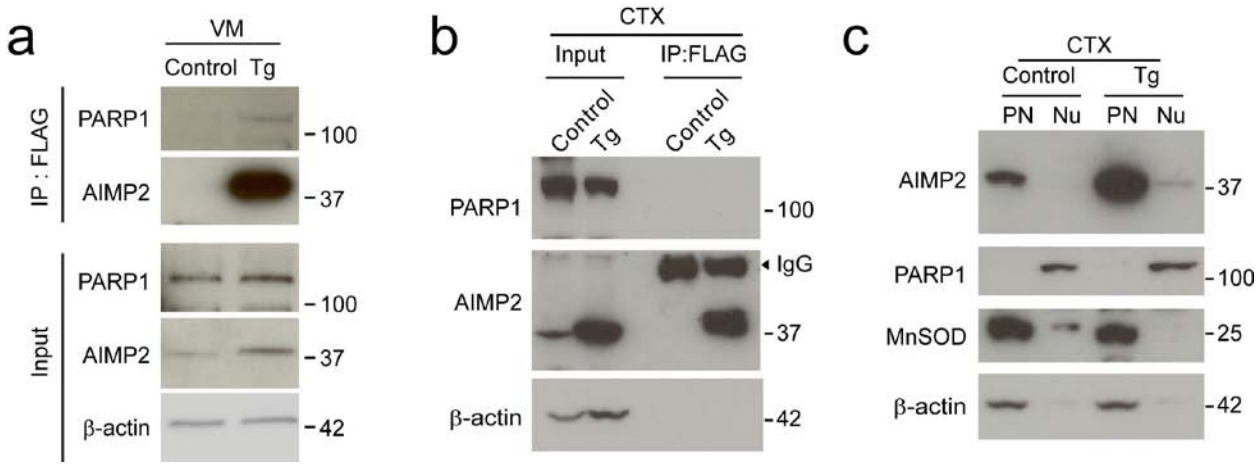


**Supplementary Fig. 6**

(a) Immunoprecipitation of AIMP2-FLAG from the ventral midbrain (VM) of control and *AIMP2* transgenic mice (line 322) monitored by western blot with antibodies to AIMP2 or PARP1. β-actin serves as a loading control.

(b) Immunoprecipitation of AIMP2-FLAG from the cortex (CTX) of control and *AIMP2* transgenic mice monitored by western blot with antibodies to AIMP2 or PARP1. β-actin serves as a loading control. Similar results were obtained in three independent experiments.

(c) Representative subcellular localization of AIMP2, and mouse endogenous PARP1 assessed in post-nuclear (PN) and nuclear (Nu) fractions prepared from the CTX of *AIMP2* transgenic and littermate control mice monitored by western blot. PARP1 serves as a nuclear marker, and MnSOD serves as a PN marker. Similar results were repeated in two independent experiments. Full length blots are presented in Supplementary Figure 14.

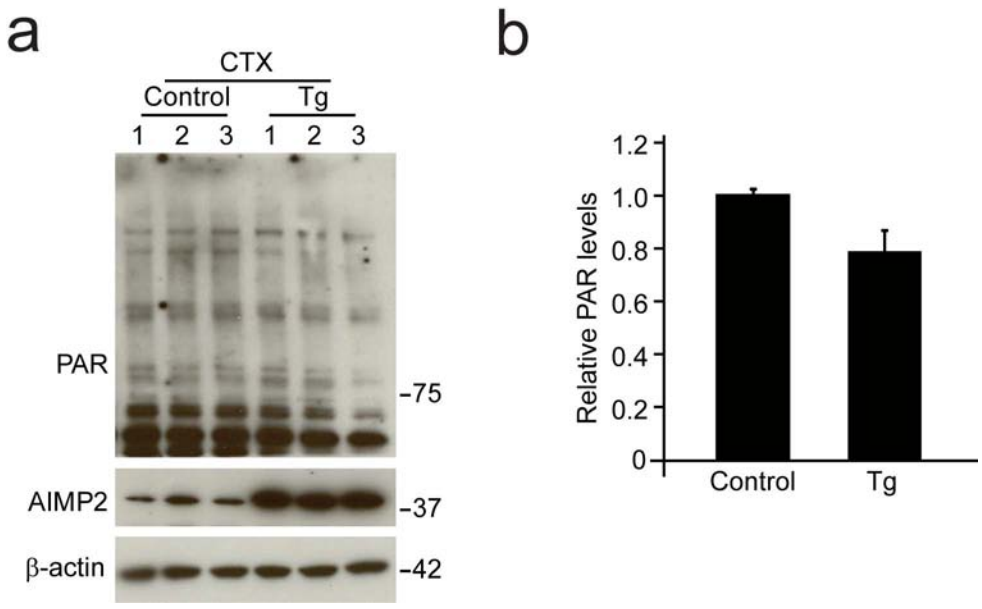


**Supplementary Fig. 7**

(a) AIMP2 and PAR from the cortex (CTX) of *AIMP2* transgenic and littermate control mice (12 month old, $n = 3$ per group) monitored by western blot.

(b) Quantification of PAR in panel (a) normalized to β-actin ($n = 3$ per group).

Quantified data are expressed as mean ± s.e.m. Full length blots are presented in Supplementary Figure 14 (a).

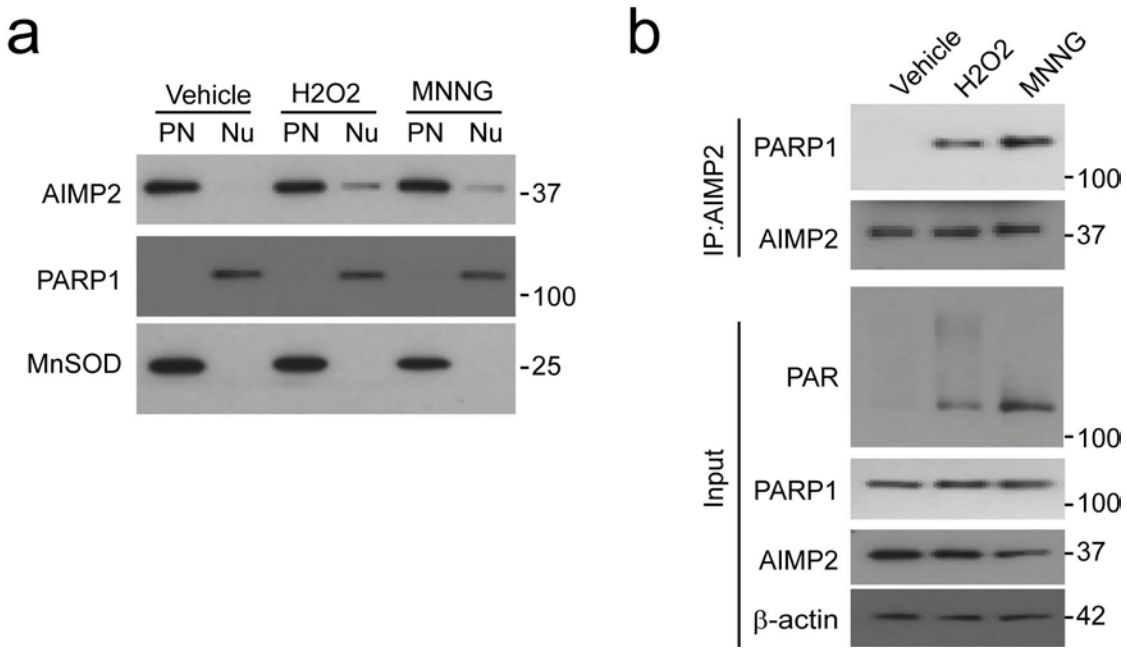


**Supplementary Fig. 8**

(a) Representative subcellular localization of endogenous AIMP2, and PARP1 assessed in post-nuclear (PN) and nuclear (Nu) fractions prepared from SH-SY5Y cells with or without treatment of $H_2O_2$ or MNNG monitored by western blot. PARP1 serves as a nuclear marker, and MnSOD serves as a post-nuclear marker. Similar results were repeated in two independent experiments.

(b) Anti-AIMP2 co-immunoprecipitation of endogenous AIMP2 and PARP1 monitored by western blot with anti-AIMP2 and anti-PARP1 antibodies in SH-SY5Y cells after treatment of $H_2O_2$ (100 μM, 15 min) or MNNG (50 μM, 15 min). PAR activation was monitored by anti-PAR antibody for input samples. β-actin serves as a loading control. Similar results were obtained in three independent experiments. Full length blots are presented in Supplementary Figure 14.

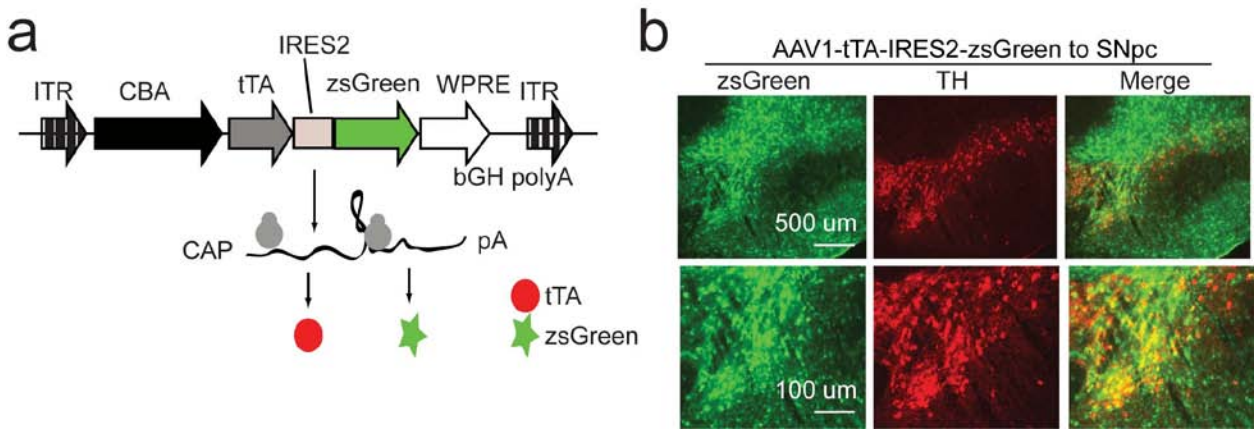


**Supplementary Fig. 9**

(a) Illustration of the AAV1-*tTA-IRES-zsGreen* viral construct with DNA elements that express tTA and fluorescent reporter zsGreen. CBA, chicken β-actin promoter. IRES2, internal ribosomal entry sequence 2. WPRE, Woodchuck Hepatitis Virus Posttranscriptional Regulatory Element. ITR, inverted terminal repeat.

(b) Representative images of TH immunofluorescence (red), zsGreen (green), and merge (yellow) from coronal sections containing the SN regions 20 days following transduction by AAV1-tTA-IRES-zsGreen in wild type mice.

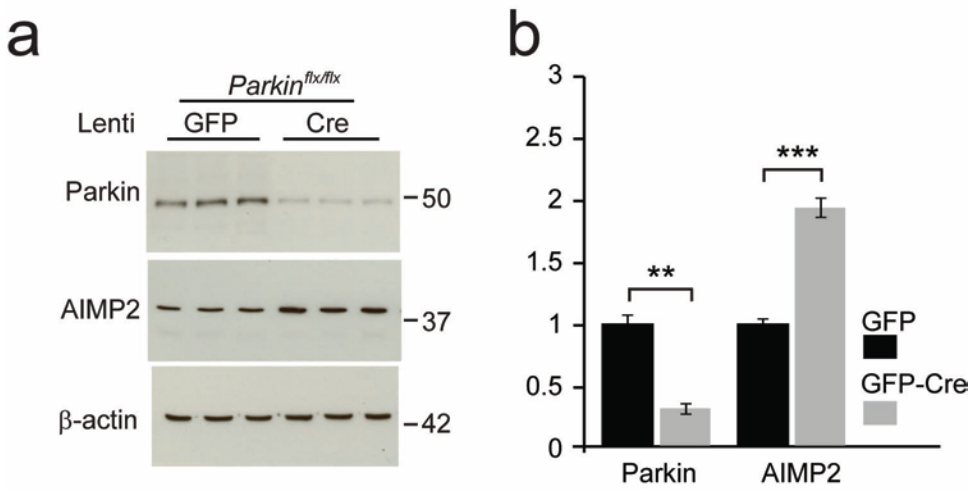


**Supplementary Fig. 10**

(a) Western blot analysis of PAR, parkin, AIMP2, and β-actin in the ventral midbrain tissues obtained 4 weeks after intranigral Lenti-GFP-Cre or Lenti-GFP injection into *Parkin* $^{flx/flx}$ mice. (b) Quantification of the levels of PAR, parkin and AIMP2 in the panel (a) normalized to β-actin. Quantified data are expressed as mean ± s.e.m., $^{**}P < 0.01$, $^{***}P < 0.001$, unpaired two-tailed Student's *t* test. n = 3 per group. Full length blots are presented in Supplementary Figure 14 (a).

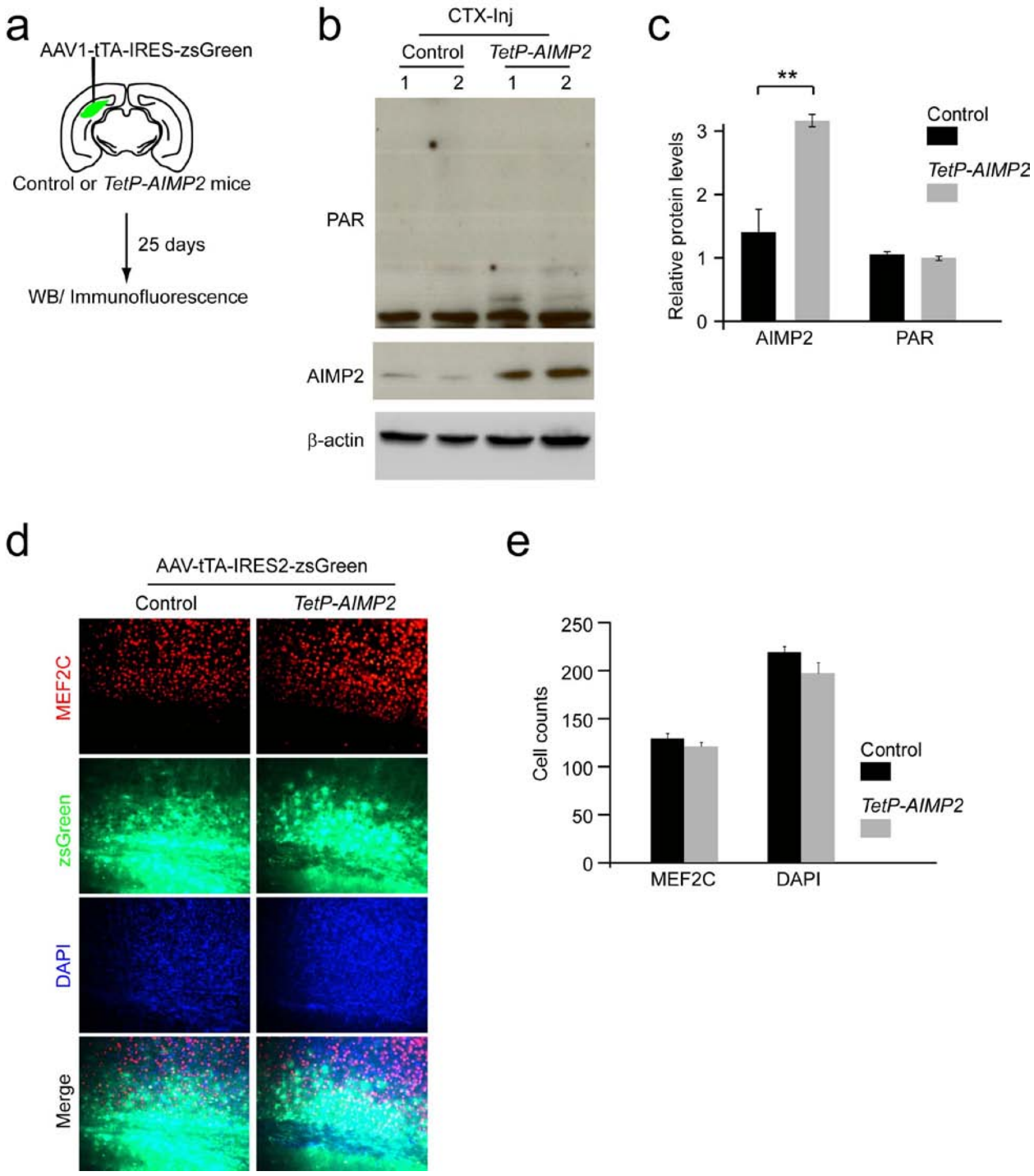


**Supplementary Fig. 11**

(a) Schematic of stereotaxic intracortical injection of AAV1-tTA-IRES-zsGreen.

(b) AIMP2 and PAR in total lysates of the cortex prepared from AAV-tTA injected sites of control and *TetP-AIMP2* mice monitored by western blot 25 days after stereotaxic intracortical injection. β-actin was used as an internal loading control.

(c) Quantification of AIMP2 or PAR levels in panel (b) normalized to β-actin (n = 4 per group)

(d) Representative immunofluorescent images of cortical sections from control and *TetP-AIMP2* mice injected with AAV-tTA-zsGreen and stained with anti-MEF2C (red) for neurons. MEF2C, Myocyte-specific enhancer factor 2C.

(e) Quantification of MEF2C positive or DAPI labeled cells in the AAV-tTA-IRES-zsGreen infected cortex from *TetP-AIMP2* mice and littermate control mice (n =3 per group)

Quantified data are expressed as mean ± s.e.m., $^{**}P < 0.01$, unpaired two-tailed Student's *t*-test (c, e). Full length blots are presented in Supplementary Figure 14 (b).

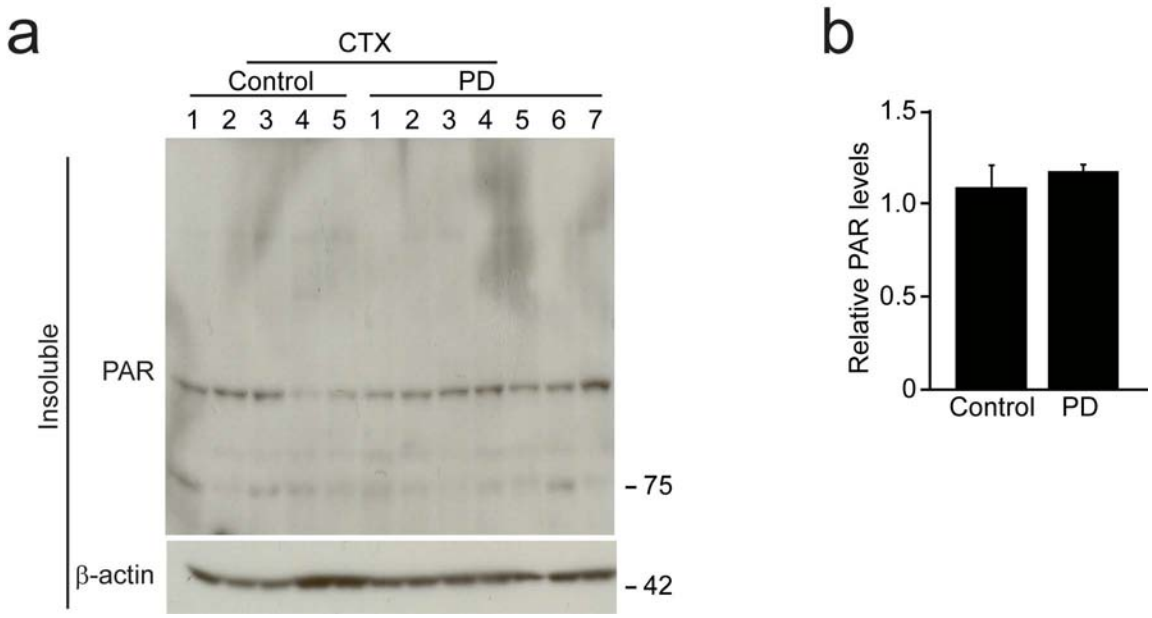


**Supplementary Fig. 12**

(a) PAR conjugated proteins in the cortex of postmortem brain tissues from PD patients and age-matched controls monitored by western blot.

(b) Quantification of PAR conjugated protein levels in panel (a) normalized to β-actin ($n$ = 5 for control subjects, and $n$ = 7 for PD). Quantified data are expressed as mean ± s.e.m., no significant difference was found between the groups in an unpaired two-tailed Student's $t$-test. Full length blots are presented in Supplementary Figure 14 (a).

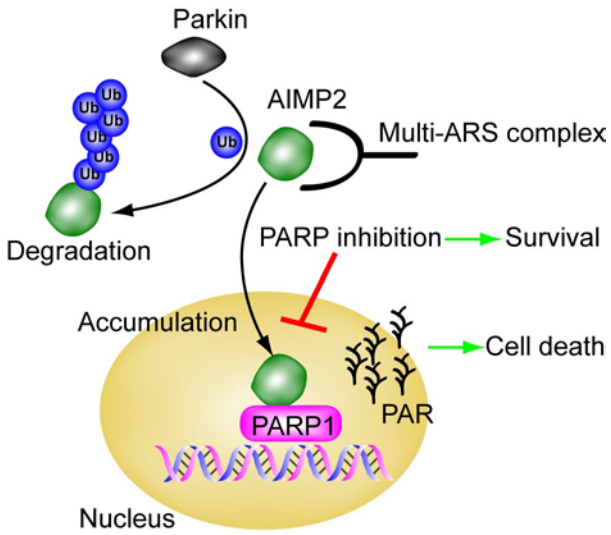


**Supplementary Fig. 13**

Schematic summary of AIMP2- PARP1 signaling pathways in Parkinson's disease pathogenesis.

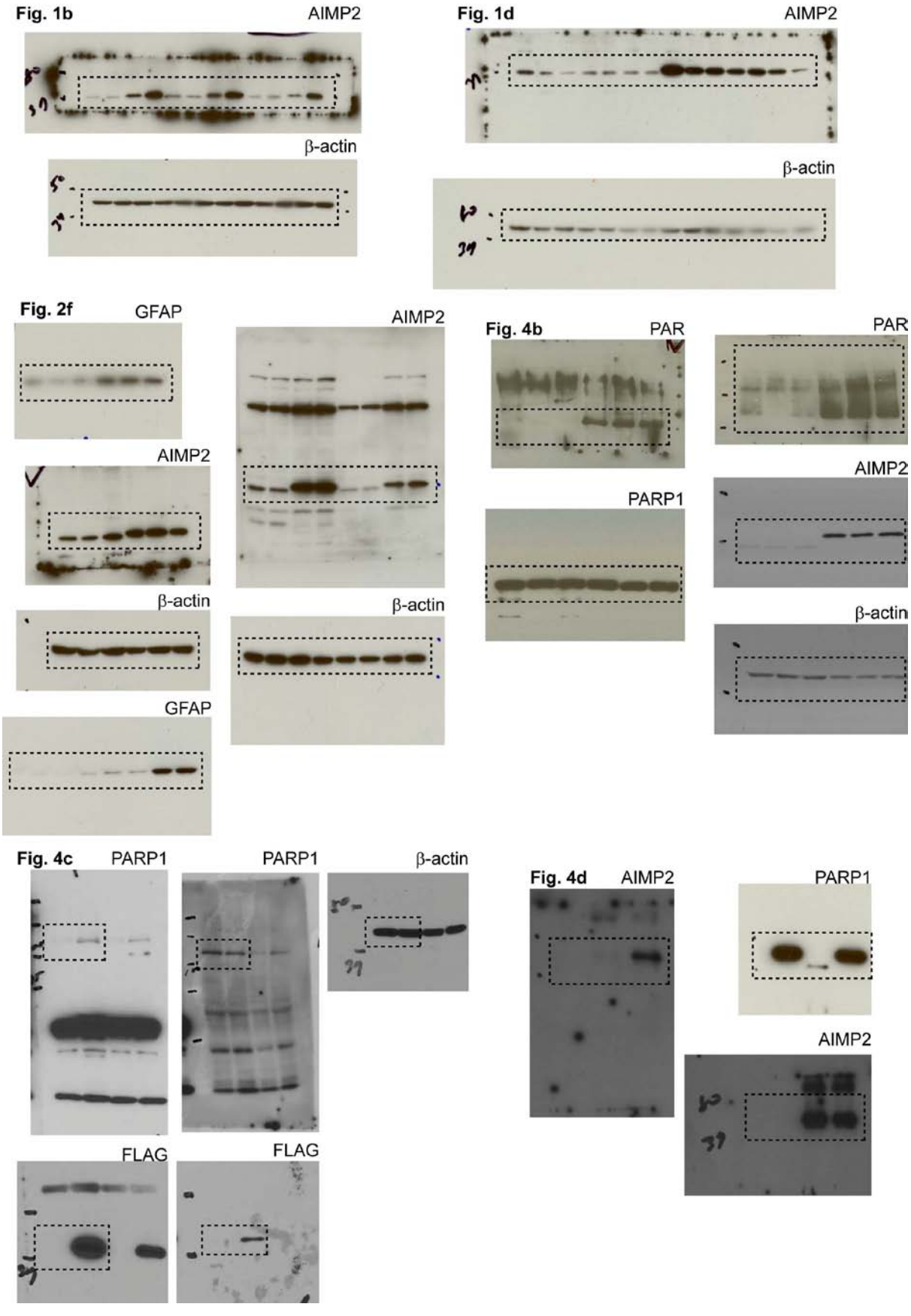
Fig. 1b
AIMP2
β-actin
Fig. 1d
AIMP2
β-actin
Fig. 2f
GFAP
AIMP2
AIMP2
β-actin
β-actin
GFAP
Fig. 4b
PAR
PARP1
PAR
AIMP2
β-actin
Fig. 4c
PARP1
PARP1
β-actin
FLAG
FLAG
Fig. 4d
AIMP2
PARP1
AIMP2

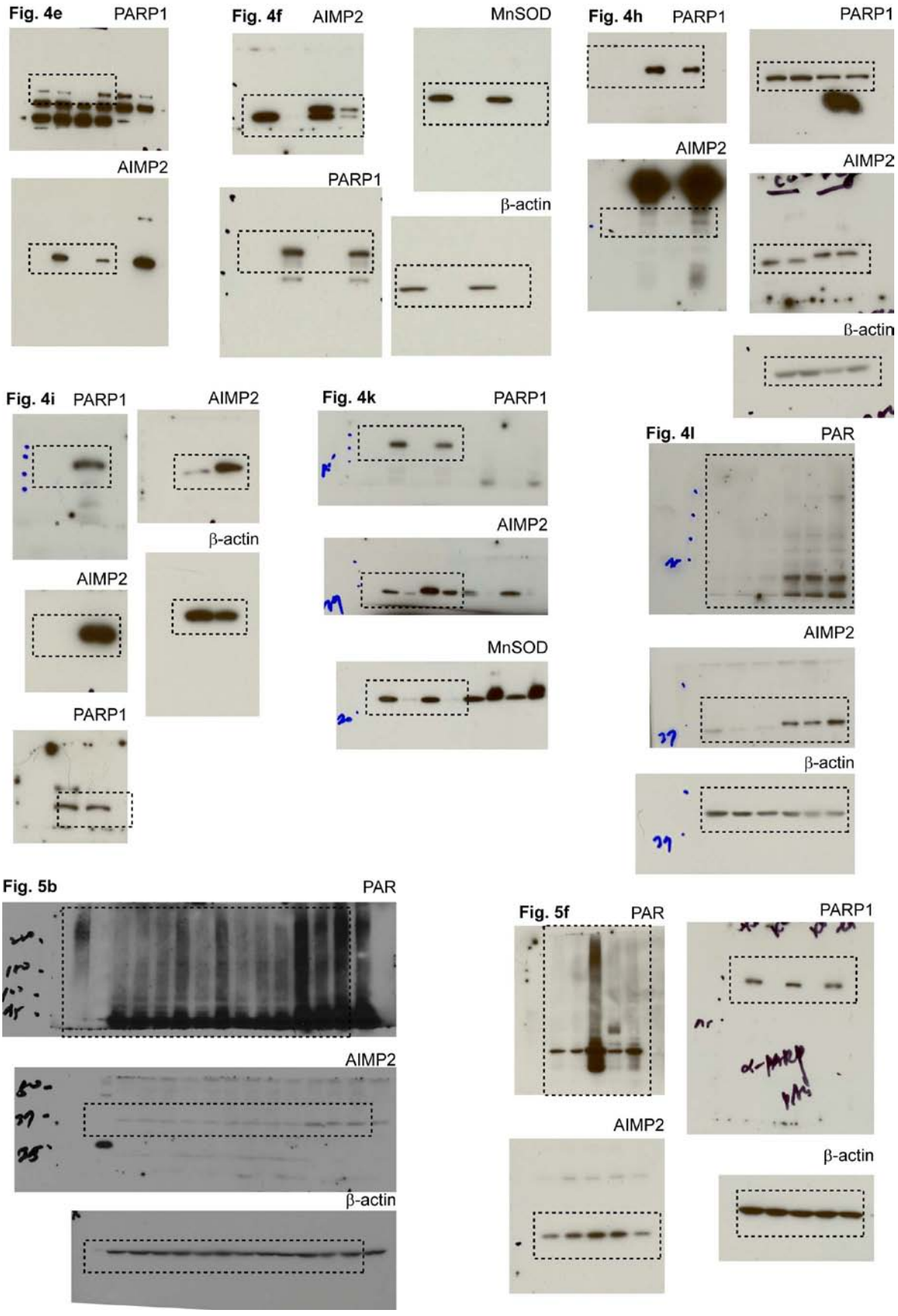
Fig. 4e
PARP1
AIMP2
Fig. 4f
AIMP2
MnSOD
PARP1
β-actin
Fig. 4h
PARP1
PARP1
AIMP2
AIMP2
β-actin
Fig. 4i
PARP1
AIMP2
β-actin
AIMP2
PARP1
Fig. 4k
PARP1
AIMP2
MnSOD
Fig. 4l
PAR
AIMP2
β-actin
Fig. 5b
PAR
AIMP2
β-actin
Fig. 5f
PAR
PARP1
AIMP2
β-actin

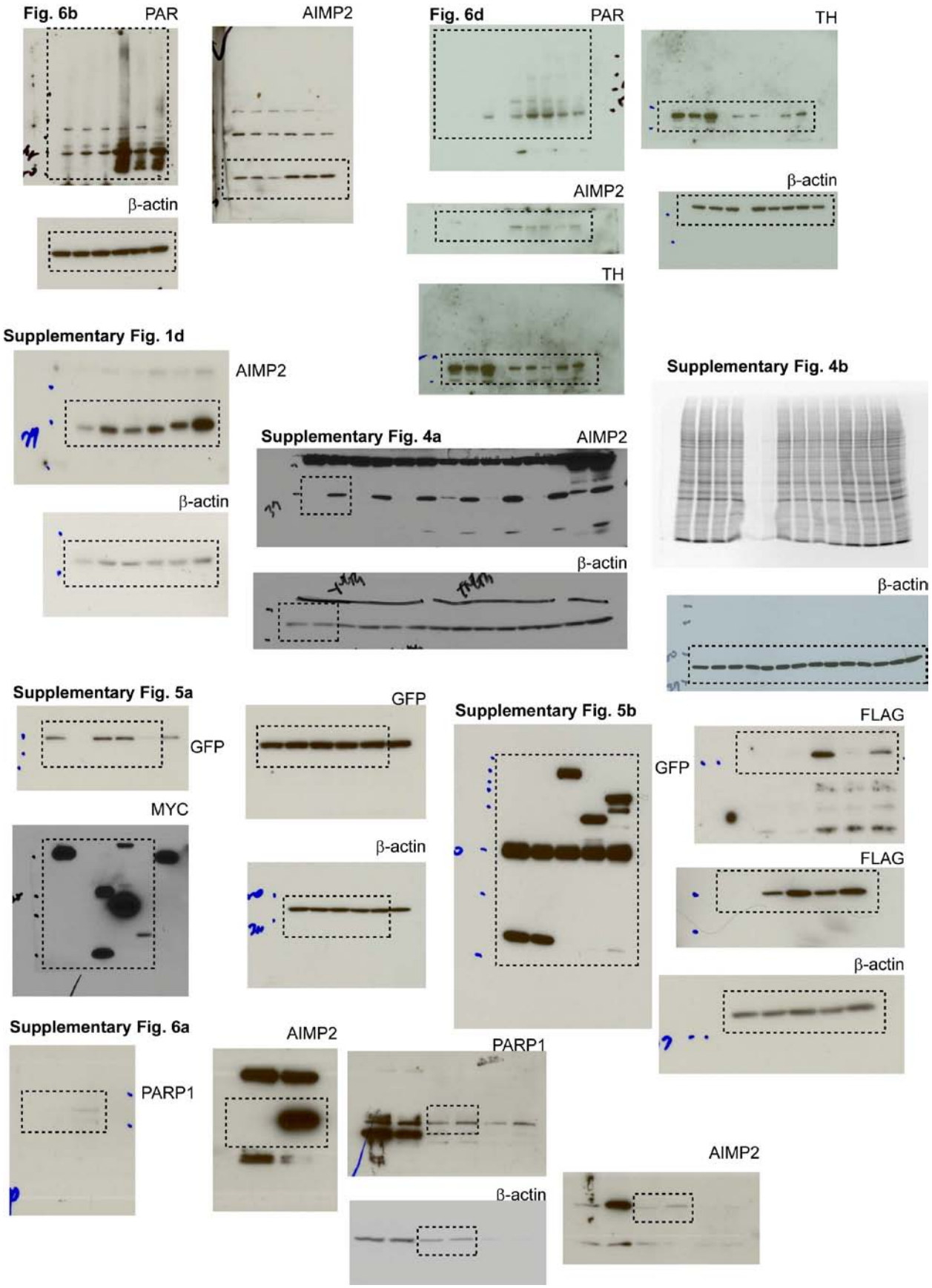
Fig. 6b
PAR
AIMP2
β-actin
Fig. 6d
PAR
TH
AIMP2
β-actin
TH
Supplementary Fig. 1d
AIMP2
β-actin
Supplementary Fig. 4a
AIMP2
β-actin
Supplementary Fig. 4b
β-actin
Supplementary Fig. 5a
GFP
GFP
MYC
β-actin
Supplementary Fig. 5b
GFP
FLAG
FLAG
β-actin
Supplementary Fig. 6a
PARP1
AIMP2
PARP1
β-actin
AIMP2

**Supplementary Fig. 6b**

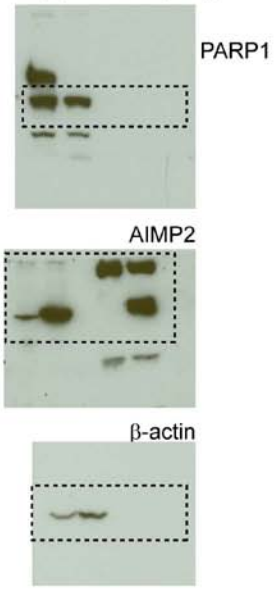


**Supplementary Fig. 6c**

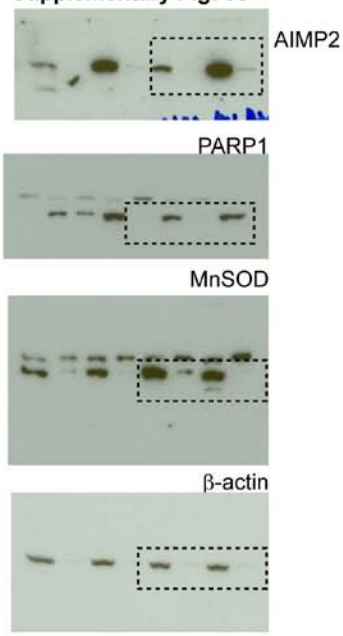


**Supplementary Fig. 7a**

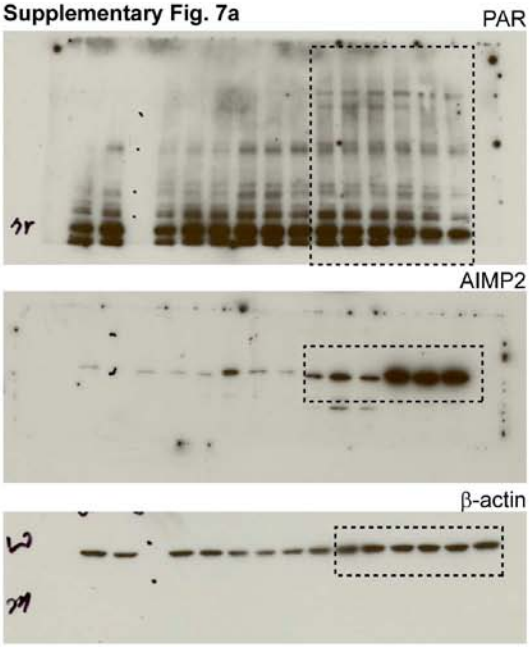


**Supplementary Fig. 8a**

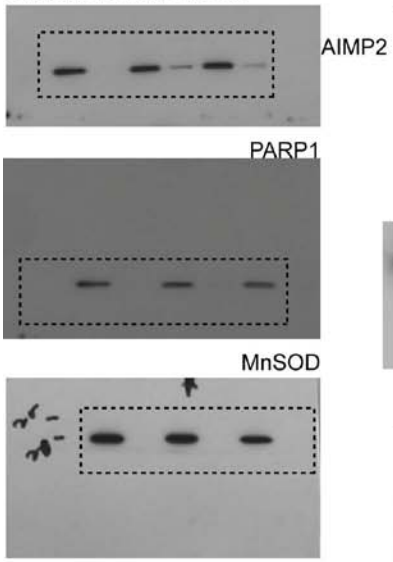


**Supplementary Fig. 8b**

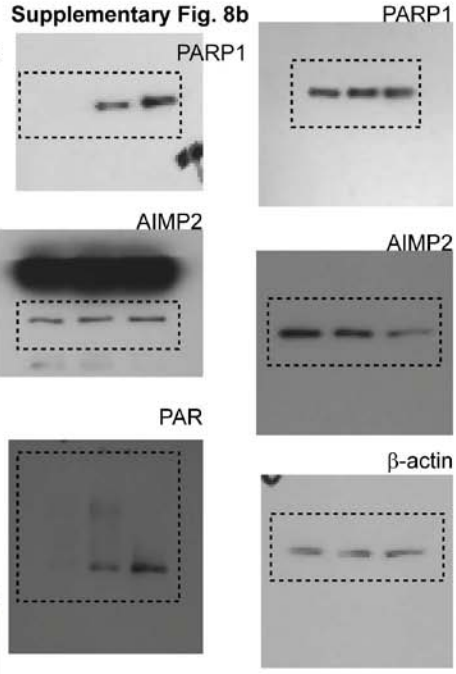


**Supplementary Fig. 10**

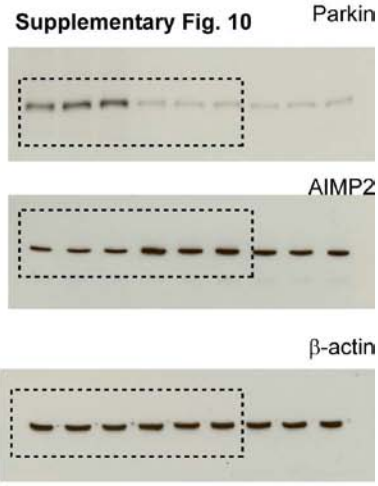


**Supplementary Fig. 11b**

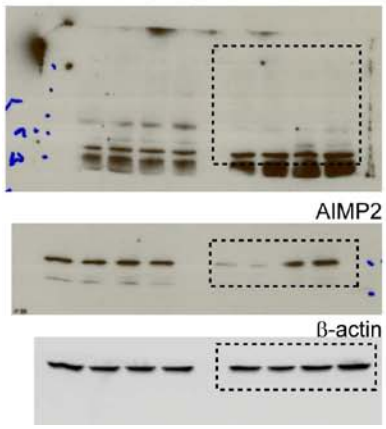


**Supplementary Fig. 12**

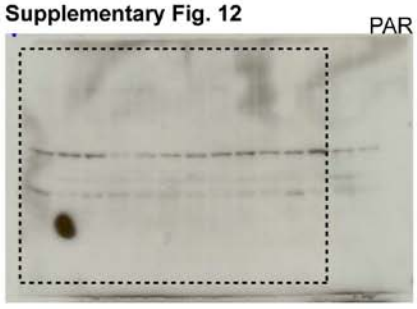

**Supplementary Fig. 14**

Uncropped images of scanned western blots. Box with dotted lines indicates cropped regions used in figures. The images are labeled to indicate the corresponding figure, panel, and antibodies.

## Supplementary Table 1. Human postmortem tissues used in Fig. 6d

| Group | Final Diagnosis | Age | Sex | Race | PMD |
|---|---|---|---|---|---|
| Control | 1. Control | 79 | M | W | 16 |
| | 2. Control | 89 | M | W | 8.5 |
| | 3. Control | 71 | M | W | 16 |
| PD | 1. PD, Neocortical | 71 | M | W | 8 |
| | 2. PD w/Dementia, Neuro. Degenn, Occipital Infarct. | 83 | M | W | 5 |
| | 3. PD w/Dementia | 76 | M | W | 17 |
| | 4. PD w/Dementia | 73 | M | W | 6.5 |
| | 5. PD, Multiple Infarcts/ Contusions-Small, Old | 80 | F | W | 6 |

Abbreviations: PD, Parkinson's disease; W, white; PMD, post-mortem delay (days).